Journal of Thermal Analysis and Calorimetry, Vol. 96 (2009) 2, 475–480

CHEMICAL STABILITY OF $Ba(Ce_{1-x}Ti_x)_{1-y}Y_yO_3$ PROTON-CONDUCTING SOLID ELECTROLYTES

P. Pasierb[*]*, Ewa Drożdż-Cieśla, R. Gajerski, S. Łabuś, S. Komornicki and M. Rękas*

AGH University of Science and Technology, Faculty of Materials Science and Ceramics, al. Mickiewicza 30, 30-059 Cracow, Poland

The purpose of this work was to investigate the influence of titanium and yttrium dopants on chemical stability of selected $Ba(Ce_{1-x}Ti_x)_{1-y}Y_yO_3$ compounds. The presented results are the part of wider research concerning the crystallographic structure, microstructure, electrical and transport properties of these groups of materials.

Samples of $Ba(Ce_{1-x}Ti_x)_{1-y}Y_yO_3$ with x=0.05, 0.07, 0.10, 0.15, 0.20, 0.30 and y=0.05, 0.10, 0.20 (for x=0.05) were prepared by solid-state reaction method. Initially, differential thermal analysis (DTA) and thermogravimetry (TG) were used for optimization of preparation conditions. Subsequently, DTA-TG-MS (mass spectrometry) techniques were applied for evaluation of the stability of prepared materials in the presence of CO_2. The X-ray diffraction (XRD) and scanning electron microscopy (SEM) results were used to determine the phase composition, structure and microstructure of materials and to assist the interpretation of DTA-TG-MS results.

The strong influence of Ti and Y dopants contents (x and y) on the properties was found. The introduction of Ti dopant led to the improvement of chemical stability against CO_2. The lower Ti concentration the better resistance against CO_2 corrosion was observed. Doping by Y had the opposite effect; the decrease of chemical stability was determined. In this case the higher Y dopant concentration the better resistance was observed. The attempt to correlate the influence of dopant on structure and chemical stability was also presented.

Keywords: *barium cerate, chemical stability, CO_2 corrosion, protonic conductors*

Introduction

In early 1980's Iwahara *et al.* [1] demonstrated that acceptor-doped strontium cerate ceramics show proton conductivity at elevated temperatures. Since then, a number of studies on proton conduction in this material have been carried out due to considerable interest for applications in hydrogen containing atmosphere gas sensors, hydrogen pumps, intermediate temperature fuel cells, steam electrolyzers etc. [2–6].

Alkaline earths cerates such as $SrCeO_3$ and $BaCeO_3$ crystallize in perovskite forms. Acceptor doping of these materials has a very slight effect on the crystal structure [7]. $BaCeO_3$ similarly as its close analogous $BaTiO_3$ is known to undergo a complex sequence of structural phase transitions. By contrast $SrCeO_3$, assuming the orthorhombic structure of the space group Pmcn undergoes no phase transition up to 1273 K [8].

Undoped $BaCeO_3$ exhibits low electrical conductivity, trivalent dopants (usually rare earth elements) in this compound play an essential role in electrical properties [9, 10]. Such ions as Y^{3+} substitute tetravalent Ce^{4+} ions and appropriate amount of oxygen vacancies are formed to maintain electroneutrality (Kröger-Vink notation was used):

$$2BaO+Y_2O_3 \leftrightarrow 2Ba_{Ba}+2Y'_{Ce}+5O_O+V_O^{\bullet\bullet} \quad (1)$$

Annealing of the obtained acceptor-doped material, $BaCe_{1-x}Y_xO_{3-x/2}$, in water vapor [11, 12] or in a hydrogen-containing atmosphere [7, 11, 13] leads to formation of protonic defects. Taking into account a small size of protons we can assume that they do not occupy lattice positions but rather attach to oxide ions forming OH groups [14]:

$$H_2O+V_O^{\bullet\bullet}+O_O^x \rightarrow 2OH^{\bullet} \quad (2)$$

$$H_2+2O_O \rightarrow 2OH^{\bullet}+2e' \quad (3)$$

The formation of OH groups has been confirmed by IR method [12, 15]. According to the reactions (2) and (3) formation of protonic defects in $BaCeO_3$-based material may change its electrical and ionic transport properties.

Among Ba- and Sr cerates, $BaCeO_3$-based ceramics shows higher total electrical conductivity. However the contribution of oxygen ions transport is rather high, especially at elevated temperatures [16]. On the other hand, the protonic transport number of acceptor doped $SrCeO_3$ is higher than that of $BaCeO_3$-based ceramics [4]. Protonic conductivity of acceptor doped $SrCeO_3$ depends on concentration of the dopant concentration. A maximum ionic conductivity of 5 mS cm^{-1} is found at x=0.1 in $SrCe_{1-x}Y_xO_{3-x/2}$ at 1073 K [17].

* Author for correspondence: ppasierb@agh.edu.pl

1388–6150/$20.00

Akadémiai Kiadó, Budapest, Hungary
Springer, Dordrecht, The Netherlands

Apart of the electrical and transport properties, the long-time stability of the protonic electrolytes is an important issue in their practical applications. There are several factors determining chemical and mechanical stability of this class of solid electrolytes such as chemical composition, structure and microstructure, operating temperature and gas phase composition.

The purpose of this work was to investigate the influence of titanium and yttrium dopants on the chemical stability of selected $Ba(Ce_{1-x}Ti_x)_{1-y}Y_yO_3$ compounds.

Experimental

Materials

In this work $Ba(Ce_{1-x}Ti_x)_{1-y}Y_yO_3$ proton-conducting solid-electrolytes with x=0.05, 0.07, 0.10, 0.15, 0.20, 0.30 and y=0.05, 0.10, 0.20 (for x=0.05) were chosen for investigations. The use of Y dopant was caused by the relatively low protonic conductivity of undoped barium cerate $BaCeO_3$, as described in the Introduction. The Ti dopant was chosen by analogy to Zr [18–20], where the improvement of chemical stability against the CO_2 was determined. Unfortunately, the introduction of Zr [18–20] as well as Ti [21] led to the decrease of total and ionic electrical conductivities. So, the search of optimum composition of $Ba(Ce_{1-x}Ti_x)_{1-y}Y_yO_3$ material from the point of view of chemical stability and electrical properties was also the one of the goals of this work.

Sample preparation

Powders of $Ba(Ce_{1-x}Ti_x)_{1-y}Y_yO_{3-\delta}$ (x=0.0–0.30, y=0.0–0.2) were prepared by solid-state reaction method. Barium carbonate $BaCO_3$ (99.9%), cerium(IV) oxide CeO_2 (99.9%), TiO_2 nanopowder (99.7%) and water solution of $Y(NO_3)_3$, all reagents supplied by Aldrich Chemical Company, Inc., were used as starting materials. After mixing the appropriate amounts of starting powders, and the impregnation by required amount of yttrium nitrate solution the materials were calcinated at 1200°C for 24 h. The general reaction of formation of barium cerium-titanium oxide can be written as follows:

$$BaCO_3+(1-x)(1-y)CeO_2+(1-y)xTiO_2+y(Y(NO_3)_3\cdot 6H_2O)\rightarrow Ba(Ce_{1-x}Ti_x)_{1-y}Y_yO_{3-y/2}+CO_2+3yNO_2+6yH_2O+yO_2 \quad (4)$$

The obtained materials were crushed in agate mortar, milled in the absolute alcohol suspension using 'Pulverisette 6' (Fritsch) mill and ZrO_2 grinding media, then formed in pellet die (∅=25 mm) at 25 MPa, isostatically pressed at 250 MPa and sintered at 1500°C for 24 h in air atmosphere. The calcination conditions were optimized basing on the XRD and DTA and TG measurements, as reported previously [21]. Obtained sintered bodies were cut to the required size and shape. All obtained materials of solid electrolytes were stored in dessicator before being used in further tests and experiments.

Methods

In this paper the results of thermal properties of materials are mainly presented. Differential thermal analysis (DTA), thermogravimetry (TG), (TA Instruments, 20° min^{-1}, measurements in synthetic air flow of 100 cm^3 min^{-1}) and mass spectrometry (MS, Balzers) techniques were applied for evaluation of the stability of prepared materials in the presence of CO_2. The X-ray diffraction (XRD, Philips X'Pert with CuK_α radiation within the 2θ range 10–90° with the scan rate of 0.008° s^{-1}) and scanning electron microscopy (SEM, NOVA NANO SEM microscope) results were used to determine the phase composition, structure and microstructure of materials and to assist the interpretation of DTA-TG-MS results.

The chemical stability of the materials against the CO_2 corrosion can be determined from the DTA, TG and MS measurements assisted with results obtained by other techniques (XRD, SEM, etc.). In this work two independent types of test were performed:

- A – exposition (saturation) of series of materials to the atmosphere containing CO_2/H_2O at room temperature (7 vol.% of CO_2 in air, 100% RH) at 22°C for 500 or 650 h,
- B – annealing of series of materials in the CO_2 dry atmosphere (100%) at 500°C for 400 h.

The first type of test corresponds to the typical storage conditions of materials or devices, while the second type of test can be representative to the working conditions of the electrochemical devices based on protonic conductors.

Samples before and after treatment A (exposition/saturation) and B (annealing) were investigated using DTA and TG coupled with mass spectrometry (DTA-TG-MS), X-ray diffraction (XRD) and scanning electron microscopy (SEM) techniques in order to determine the influence of Ti and Y dopants on the stability of the materials.

Results and discussion

Crystallographic structure, phase composition and microstructure

Figure 1 shows the SEM image of typical microstructure of $BaCeO_3$ sample. As can be seen dense materials with some apparent porosity were obtained with average grain size of several μm. The influence of

Ti and Y dopant on microstructure was hardly observable. It is interesting to mention, that the discriminated 'decoration' of some of the grains, probably by secondary carbonates was observed. The difference of the 'decoration' degree of grains may be explained by different concentration of nucleation centers caused by various orientations of individual grains.

Basing on the XRD results presented previously [21], it can be stated that undoped sample (x=0, y=0) crystallized in orthorhombic Pmcn structure, while the incorporation of titanium into the lattice lead to a gradual ordering of the structure, which was observed as a disappearance of the reflex splitting with the increase of Ti concentration. Also, the shift of reflex maxima towards higher values of 2θ with the increase of Ti is observed, caused by the decrease of lattice constants. Detailed crystallographic studies are under the way, the results will be published later.

In case of of yttrium doped samples the constant Ti concentration (x=0.05) was chosen and different Y dopant concentrations were used, up to y=0.20. Figure 2 shows the comparison of XRD spectra for the selected samples doped with yttrium.

It was observed that the structure gradually changes from tetragonal to regular form with increasing content of yttrium, and no additional phases were detected up to y=0.20.

Resistance against the CO_2

As reported previously [22] the $BaCeO_3$ based materials during the corrosion tests turned partially into barium carbonate and cerium oxide. Figure 3 shows the TG results of samples before the exposition (saturation) and annealing tests.

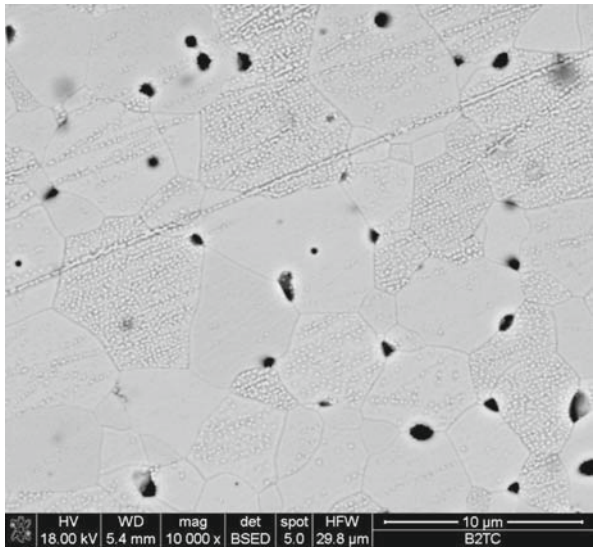

Fig. 1 SEM image of polished surface of $BaCeO_3$ sintered body (1500°C/12 h). Magn.: 10000×

As can be seen only minor mass loss, not exceeding 0.3%, can be detected in these as-prepared samples. Doping by yttrium led to the increase of mass loss comparing to undoped and Ti-doped materials. It can be understood basing on the results of mass spectrometry measurements of the gases evolved during the DTA-TG measurements, as presented in Fig. 4 for the sample with the highest concentration of yttrium dopant used. It was found that the observed mass loss was caused predominantly by the dissapperance of protonic defects at about 600–800°C. According to the point defect model presented in Introduction part, the introduction of yttrium leads to the increase of the oxygen vacancies and thus protonic defects concentrations.

Figures 5 and 6 show the TG and MS results of Ti-doped materials after the exposition in CO_2 rich atmospheres (25°C/100% RH/7% CO_2/650 h).

As can be deducted from the results presented in Figs 5 and 6, the mass loss was caused by the release of water vapour at temperature below 200°C and in the range of 400–600°C due to destruction of protonic defects, followed then by the release of carbon dioxide above 900°C.

The introduction of titanium into the lattice led to the improvement of the chemical stability of the

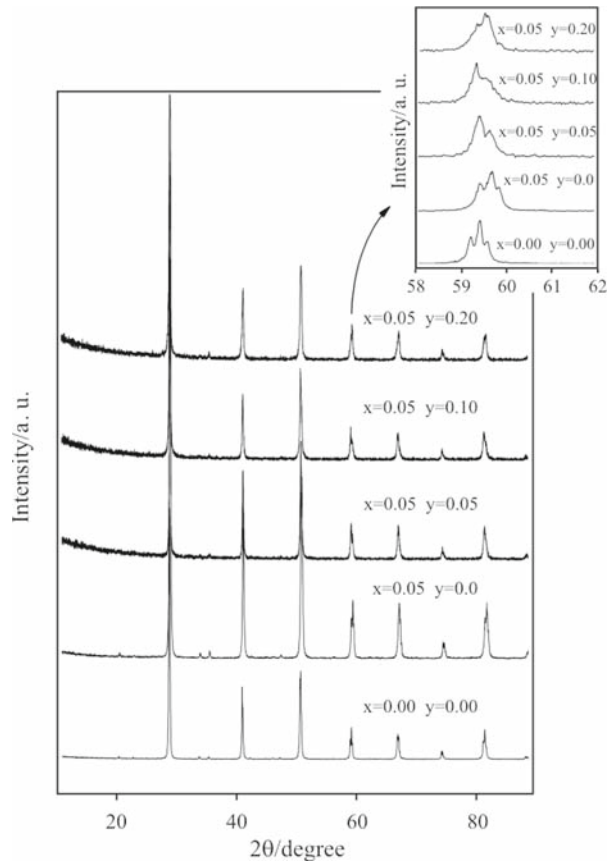

Fig. 2 XRD of example $Ba(Ce_{1-x}Ti_x)_{1-y}Y_yO_3$ samples. The inset shows the evolution of one of the reflexes

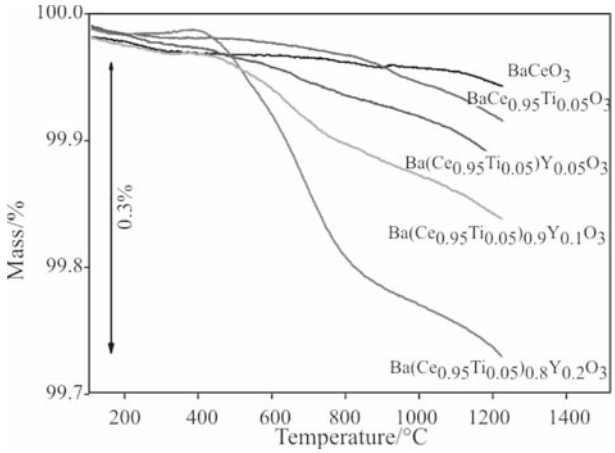

Fig. 3 TG results of $Ba(Ce_{1-x}Ti_x)_{1-y}Y_yO_3$ as-prepared sintered bodies, before the exposition and annealing tests

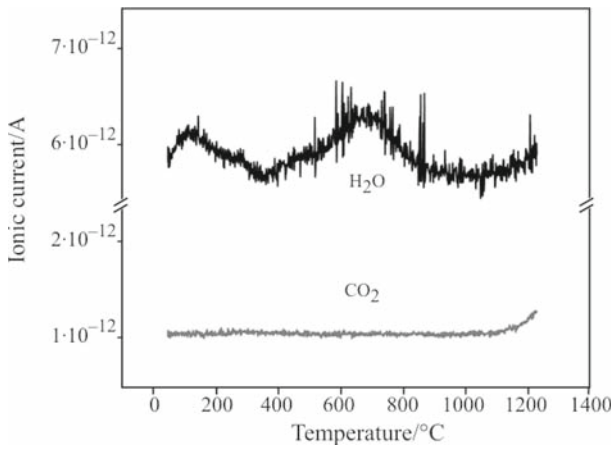

Fig. 4 Mass spectrometry measurements of $Ba(Ce_{0.95}Ti_{0.05})_{0.8}Y_{0.2}O_3$ sample before the exposition and annealing tests

materials. As can be noticed, the use of smallest amount of Ti dopant (x=0.05) led to the best results; practically no mass loss of this sample after this corrosion test was detected. The higher Ti dopant concentration the worse chemical resistance to the presence of CO_2 was observed, but in any case the obtained results were better comparing to the undoped sample (x=0) and much better comparing to the yttrium doped samples, as shown in Fig. 7.

As can be seen doping by Y leads to the decrease of chemical stability against the CO_2 comparing to the undoped and Ti-doped samples. The dependence of mass loss magnitude on the yttrium dopant concentration is not monotonic; the worst properties were observed for sample with y=0.1, while further doping (y=0.2) led to the improvement of resistance against CO_2, even compared to the sample with y=0.05.

The observed improvement of chemical stability after doping with Ti and Y may be in general correlated to the ordering of the crystallographic structure, as reported previously in literature [23, 24]. It was

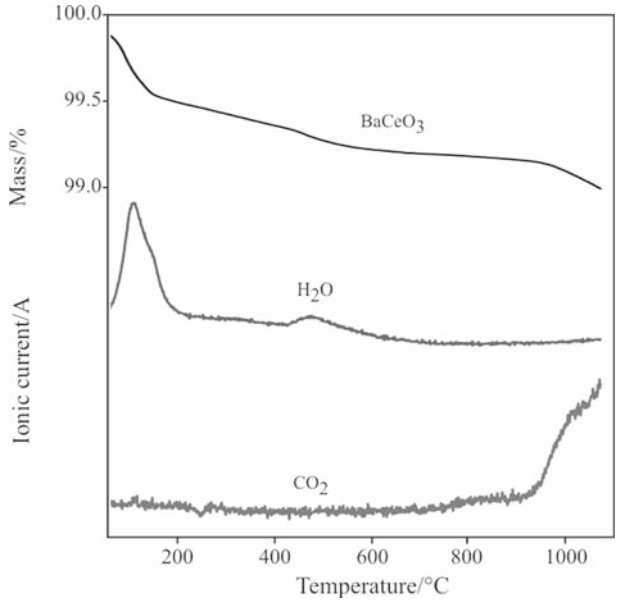

Fig. 5 TG results of $BaCe_{1-x}Ti_xO_3$ sintered samples after extended treatment in CO_2/H_2O rich atmospheres (25°C/100% RH/7% CO_2/650 h)

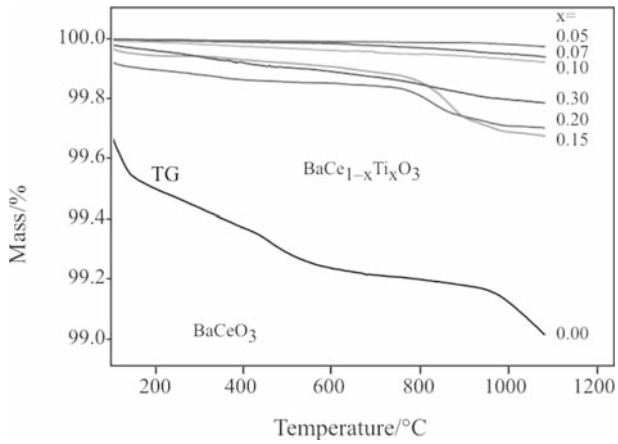

Fig. 6 TG and mass spectrometry measurements of $BaCeO_3$ sample after extended treatment in CO_2/H_2O rich atmospheres (22°C/100% RH/7% CO_2/650 h)

found that the enthalpy of formation of perovskites from individual oxides, (which can be used for further calculations and associated with the stability of perovskites in the presence of CO_2) shows the linear correlation with the perovskite Goldschmidt tolerance factor, t, defined as:

$$t = \frac{(r_A + r_B)}{[\sqrt{2}(r_B + r_O)]} \quad (5)$$

where r_A, r_B, r_O are the ionic radius of A, B and O atoms in ABO_3 perovskite.

This structural parameter describes the extent of distorsion of the perovskite structure from ideal cubic structure due to dismatch between A–O and B–O bond lengths. The higher t factor value the more nega-

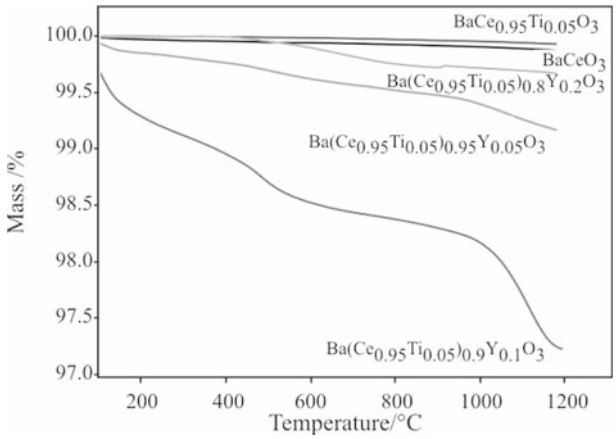

Fig. 7 Comparison of TG results obtained for $Ba(Ce_{1-x}Ti_x)_{1-y}Y_yO_3$ samples after extended treatment in CO_2/H_2O rich atmospheres (22°C/100% RH/7% CO_2/500 h)

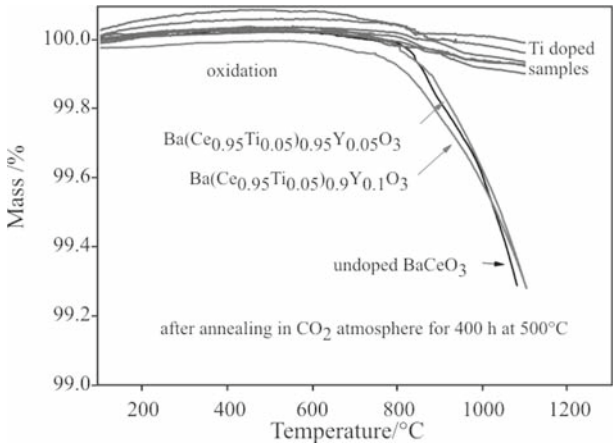

Fig. 8 TG results measured for the $Ba(Ce_{1-x}Ti_x)_{1-y}Y_yO_3$ samples after extended annealing in CO_2 atmosphere (500°C/100% CO_2/400 h)

tive entalpy of formation was observed and thus better stability was expected.

Figure 8 shows the results of TG measurements of $Ba(Ce_{1-x}Ti_x)_{1-y}Y_yO_3$ sintered samples after annealing in CO_2 atmosphere at 500°C for 400 h.

As can be noticed the materials have separated into two groups where almost the same mass losses were observed. The first group consists of the Ti-doped materials, while the second group contains the undoped and yttrium doped $BaCeO_3$ materials. The Ti doped samples remained stable, as expected basing on the results presented above. From the other hand the long-term annealing CO_2 tests did not allowed to determine the influence of the yttrium dopant concentration on the resistance against CO_2. Samples exhibit the same mass loss which suggests that the secondary carbonates were formed rather during cooling down the samples than during the isothermal heating. These results indicate that further tests involving heating-cooling cycles are necessary to get some practical information concerning the durability of such materials in real working conditions, where the temperature and atmosphere changes are present.

In case of all samples the slight mass increase in temperatures up to 800°C may be observed which can be explained by the simultaneous oxidation of material during the measurement.

Conclusions

In this work the results concerning the influence of Ti and Y dopant (for selected Ti dopant concentration x=0.05) on chemical stability of $Ba(Ce_{1-x}Ti_x)_{1-y}Y_yO_3$ solid electrolytes in the presence of CO_2 and H_2O were discussed. The investigated materials were prepared by solid-state reaction method which allowed to obtain dense, uniform bulk materials. Basing on XRD measurements it was found that doping by both Ti and Y leads to the structure ordering, the gradual changes from orthorhombic to even regular form with increasing content of titanium or yttrium dopant are observed.

Basing on the DTA-TG-MS measurements of the samples before and after the tests with CO_2 it was found that the introduction of Ti dopant leads to the improvement of chemical stability against CO_2. The lower Ti concentration the better resistance was observed. Doping by Y had the opposite effect – the decrease of chemical stability was determined in this case, as expected. But, the higher Y dopant concentration the better resistance to CO_2 corrosion was determined.

The observed improvement of chemical stability after doping with Ti and Y may be generally correlated to the ordering of the crystallographic structure, as reported previously in literature.

Basing on the previously published results concerning the electrical and transport properties of $Ba(Ce_{1-x}Ti_x)_{1-y}Y_yO_3$ compounds [21] and the results of this work the optimal composition of the material for the construction of different electrochemical devices may be proposed at this stage of investigation. The $Ba(Ce_{0.95}Ti_{0.05})_{0.8}Y_{0.2}O_3$ seems to be the most promising material from the point of view of reasonably high electrical conductivity, high protonic transference number and acceptable chemical stability in the presence of CO_2.

Acknowledgements

The financial support of Polish Ministry of Education and Science (MEiN), Project No. PBZ-KBN-117/T08/03 is acknowledged.

References

1 H. Iwahara, T. Esaka, H. Uchida and N. Maeda, Solid State Ionics, 34 (1981) 359.
2 N. Bonanos, K. S. Knight and B. Ellis, Solid State Ionics, 79 (1995) 161.
3 T. Yajima, K. Koide, H. Takai, N. Fukatsu and H. Iwahara, Solid State Ionics, 79 (1995) 333.
4 H. Iwahara, Solid State Ionics, 86–88 (1996) 9.
5 F. L. Chen, O. T. Sørensen, G. Y. Meng and D. K. Peng, J. Thermal. Anal., 49 (1997) 1255.
6 N. I. Matskevich, J. Therm. Anal. Cal., 90 (2007) 955.
7 K. S. Knight and N. Bonanos, Mater. Res. Bull., 30 (1995) 347.
8 J. Ranlov and K. Nielson, J. Mater. Chem., 4 (1994) 867.
9 H. Iwahara, T. Esaka and H. Uchida, Solid State Ionics, 3/4 (1981) 359.
10 H. Iwahara, H. Uchida, K. Ono and K. Ogaki, J. Electrochem. Soc., 135 (1988) 529.
11 N. Bonanos, Solid State Ionics, 53/56 (1992) 967.
12 T. Yaima and H. Iwahara, Solid State Ionics, 50 (1992) 281.
13 I. Kosacki, J. G. M. Becht, R. van Landschoot and J. Schoonman, Solid State Ionics, 59 (1993) 287.
14 T. Norby, Solid State Ionics, 40/41 (1990) 849.
15 J. F. Liu and A. S. Nowick, Solid State Ionics, 50 (1992) 131.
16 N. Bonanos, B. Ellis and M. N. Mahmood, Solid State Ionics, 44 (1991) 305.
17 R. J. Phillips, N. Bonanos, F. W. Poulsen and E. O. Ahlgren, Solid State Ionics, 125 (1999) 389.
18 K. H. Ryu and S. M. Haile, Solid State Ionics, 125 (1999) 355.
19 K. Katahira, Y. Kohcki, T. Shimura and H. Iwahara, Solid State Ionics, 138 (2000) 91.
20 W. Munch, K. D. Kreuer, G. Seifert and J. Maier, Solid State Ionics, 136/137 (2000) 183.
21 P. Pasierb, E. Drożdż-Cieśla and M. Rekas, J. Power Sources, 181 (2008) 17.
22 P. Pasierb, Annales de Chimie – Science de Matériaux, 33 (2008) 157.
23 E. Takayama-Muromachi and A. Navrotsky, J. Solid State Chem., 72 (1988) 244.
24 S. M. Haile, G. Staneff and K. H. Ryu, J. Mater. Sci., 36 (2001) 1149.

Received: December 2, 2008
Accepted: December 12, 2008
Online First: April 13, 2009

DOI: 10.1007/s10973-008-9829-x